Available online at www.sciencedirect.com
SCIENCE DIRECT®
Journal of Photochemistry and Photobiology A: Chemistry 172 (2005) 7–17
Journal of Photochemistry and Photobiology A:Chemistry
www.elsevier.com/locate/jphotochem

Photophysics of mesoporphyrin IX in solution and confined in sol–gel-derived matrices

Mário Rui Pereira, João A. Ferreira, Graham Hungerford*

Departamento de Física, Universidade do Minho, Campus de Gualtar, 4710-057 Braga, Portugal

Received 13 July 2004; received in revised form 5 November 2004; accepted 5 November 2004
Available online 8 January 2005

Abstract

In this work we investigate both the stationary and transient spectroscopic properties of mesoporphyrin IX when incorporated into porous matrices produced using the sol–gel technique. These matrices were produced using both titanium and silicon containing precursors to form solid glassy monoliths, with the addition (in some samples) of DMF as a drying control chemical additive. Steady state and time-resolved fluorescence measurements were performed on the freshly gelled and finished matrices and comparison with solution studies made. The latter show a dependence of the mesoporphyrin absorption and emission spectra with refractive index and also with the $E_{T(30)}$ solvent scale. Anomalies are encountered with both aprotic and protic solvents, respectively, when using these scales, indicating interaction with nitrogens in the pyrrole ring. The effect of pH is also clear and the presence of the cationic and dicationic forms of the porphyrin observed via steady state and time-resolved measurements, both in solution and with the porphyrin incorporated within the matrix pore structure where an estimate of refractive index and $E_{T(30)}$ value were made. With time the porphyrin was found to aggregate and degrade within the matrix environment, although differences were encountered between the various matrix forms.

Keywords: Mesoporphyrin IX; Fluorescence; Sol–gel; Solvent effects

1. Introduction

Porphyrins in general have attracted considerable attention in many areas of investigation because of their spectral properties [1,2]. They present a characteristic absorption spectrum consisting of an intense (*Soret* or *B*) band close to 400 nm and less intense (*Q*) bands in the region 500–600 nm, while their fluorescence emission usually consists of two distinct bands in the region 600–700 nm. Indeed, as well as innumerable articles, there is a whole series of books [3] devoted to this class of molecules. Interest in them stems from their biological applications, as they are encountered in many entities such as chlorophyll and haemoglobin, as well as being found in enzymes. Porphyrins have also been employed in photodynamic therapy [4] and are produced in the body from aminolevulinic acid, which is used in the manufacture of heme [5]. This has also prompted research on their incorporation and localisation in membranes [6]. Because of their spectral and electronic properties attention has also turned to their application for solar energy conversion when used in conjunction with TiO_2 matrices [7,8]. In both biological and solar energy applications it is important to ascertain the photophysical properties of porphyrins when incorporated into microheterogeneous media, as these can be different to those in homogeneous media. Owing to their interaction with the confining media, as in the case of photosensitisation of TiO_2, for example, obtaining data on the process of charge injection is of great importance.

In this study we investigate mesoporphyrin IX (MP), the structure of which is given in Fig. 1. This porphyrin has been found to exhibit changes in its spectral properties when it is incorporated into membranes and proteins [6,9,10]. Because of the presence of the two pyrrole nitrogens, which have the

* Corresponding author. Tel.: +351 253604320; fax: +351 253678981.
E-mail address: graham@fisica.uminho.pt (G. Hungerford).

1010-6030/$ – see front matter © 2004 Elsevier B.V. All rights reserved.
doi:10.1016/j.jphotochem.2004.11.003

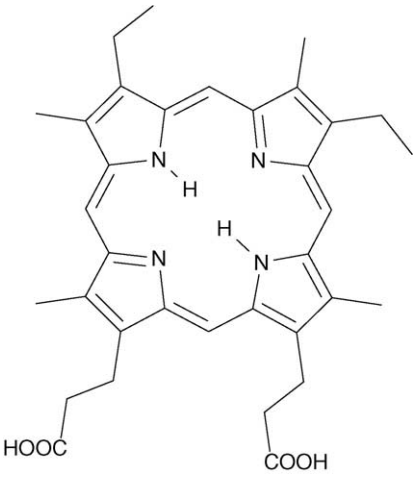

Fig. 1. Structure of mesoporphyrin IX.

possibility of gaining protons, and the two propionic acid residues, that can dissociate, this molecule can exist as different ionic forms depending of the pH of the environment [11]. Although spectral changes accompany the ionisation of the nitrogens, the major influence of pH on the propionic acid residues may relate to changes in fluorescence intensity because of alterations in solubility [12], with no changes in spectral shape. The presence of carboxylate groups also allows it to bind to nanocrystalline TiO_2, where charge injection has been reported [7]. Thus we choose MP for incorporation into both titania (active system for charge injection) and silica (passive system) matrices produced using the sol–gel technique [13]. We have previously demonstrated that these porous glassy matrices provide good hosts for the incorporation of dyes [14] and that the environment can be tuned by the addition of solvents [15], which can also be employed as drying control chemical additives (DCCAs) to prevent stresses and cracking during matrix production. In this work we present both stationary and transient fluorescence, along with absorption studies of MP in the sol–gel systems to elucidate its photophysical properties in relation with the confinement in these ordered media and possible charge injection. A complementary study in solution was also performed to ascertain its behaviour in component solvents of the sol–gel systems and to help assess the environment effects in the matrices.

2. Experimental

2.1. Matrix production

The titania matrices were prepared in a similar manner to that we have previously reported [14], while the silica ones were either produced using a method given beforehand [14] or adapted from that described by Flora and Brennan [16]. For ease of measurement the matrices were produced in monolith form using 10 mm pathlength plastic cuvettes as moulds. Doping with MP was either performed during the initial reaction procedure or from ethanol solution after the gelling stage and during the drying process. A matrix was judged finished when no further shrinkage was observed and it appeared to be physically robust with good optical properties. All solvents used were of spectroscopic grade and MP (7,12-diethyl-3,8,13,17-tetramethyl-21H,23H-porphin-2,18-dipropionsäure IX dihydrochloride) was obtained from Sigma–Aldrich GmbH and used as received.

2.2. Measurements

Stationary measurements were performed using Shimadzu UV-3101PC (absorption) and SPEX Fluorolog (fluorescence) spectrophotometers. A list of the solvents used for the solution study is given in Table 1. Time-resolved measurements were carried out using a single-photon counting apparatus equipped with LED excitation sources with peak emissions at 495 and 560 nm (IBH NanoLED). The nominal full width at half maximum was about 1.4 ns. The fluorescence emission was wavelength selected using filters and detected with a Hamamatsu R2949 side window photomultiplier. Data analysis was performed with IBH DAS6 software and the goodness of fit judged in terms of a χ^2 value and weighted residuals. The errors on the lifetimes (τ_i) are given as three standard deviations and the pre-exponential factors (α_i) are given normalised to unity.

3. Results and discussion

As a basis to help analyse the matrix data a study in solution was conducted. As the matrix forming reaction involved the presence of an acid catalyst the effect of pH was investigated. This was performed in aqueous solution and also the effect of acid on MP in ethanol was monitored, as this is a major solvent in our sol–gel route. The matrix interior has been reported as having several environments [16] and the spectra of MP were recorded in a variety of solvents of differing

Table 1
Solvents used in the solution study

Solvent	$(n^2-1)/(2n^2+1)$	$E_{T(30)}$ (kcal mol^{-1})
Methanol (1)	0.169	55.4
Acetonitrile (2)	0.175	45.6
Acetone (3)	0.180	42.2
Ethanol (4)	0.181	51.9
Isopropanol (5)	0.186	48.4
1-Butanol (6)	0.195	50.2
Tetrahydrofuran (7)	0.196	37.4
Dioxane (8)	0.203	36.0
1-Heptanol (9)	0.203	–
Dimethylformamide (10)	0.206	43.8
Dimethylsulfoxide (11)	0.221	45.1
Toluene (12)	0.226	33.9
Isopropoxide (13)		

dielectric constants. The purpose of these studies was to gain information concerning the porphyrin environment within the matrix. By the use of the two different matrix materials it was hoped to elucidate any electron transfer behaviour (the silica system would act as a reference). MP has been shown to couple to nanocrystalline TiO_2 and a photocurrent action spectrum has been measured [7]. There are reports that the absence of conjugation of the coupling carboxyl groups with the π electron system does not affect electron injection [7], while the relative energy levels of the sensitiser and matrix are not the main factor controlling the efficiency of charge injection [17]. In this discussion the term neutral monomer form will be used to indicate the lack of charge on the core nitrogens (i.e. ignoring any changes on the carboxylate groups).

3.1. Solution studies

MP is regarded as hydrophobic and is found to aggregate in aqueous solution [18] and a dimerisation constant of $5.4 \times 10^6\ M^{-1}$ has been reported [19]. The calculated spectrum for the dimer exhibits a blue shifted and broadened *Soret* band accompanied by changes in the *Q* region along with the presence of an extra emission band [20]. Aggregation can be reduced by addition of small quantities of ethanol [18] or by addition of acid, which causes protonation of the pyrrole core nitrogens making the molecule less hydrophobic [6]. The presence of cationic forms of mesoporphyrin IX ester (MPE) has been previously ascertained from its absorption spectrum and is manifest by a reduction in the number of *Q* bands accompanied by a change in *Soret* band position [21].

To solubilise MP in aqueous solution the porphyrin was first dissolved in ethanol and most of the solvent evaporated before the addition of water. It is estimated that the final solution contained considerably less than 0.5% of ethanol by volume. However the presence of acid (37% HCl) was required to be able to obtain a measurable spectrum and this, for different pH values, is shown in Fig. 2. In these absorption spectra clear changes are observed on lowering the pH and the presence of isobestic points at 539 and 563 nm discerned (from overlaying the spectra). Before the addition of acid the (mainly) aggregated MP exhibited two broad bands centred about 349 and 452 nm, as well as a band at 521 nm in the *Q* region. After addition the Soret band located at 399 nm grows in, indicating the porphyrin disaggregating and at a pH of 2.2 three main bands in the *Q* region are observed. These are at 523 nm with a shoulder at 548 nm, with others at 579 and 628 nm. On increasing acidity the 523 nm band drastically diminishes while the shoulder increases slightly and is manifest as a band. That at 579 nm decreases and another band at 589 nm becomes evident while the longer wavelength band (at 628 nm) diminishes. This behaviour can be attributed to a transition from an aggregated form to a mixture of cation and dication [21], with a significantly larger quantity of dication present at the lowest pH. However the position of the *Soret* band (399 nm) is that previously reported for the monomer in aqueous solution, with the dication absorbing at 404 nm [21]. In that study, surfactants were added to solubilise the porphyrin, but other work in buffered solution has reported a lower value (392 nm) [10]. As our *Q* bands are also at slightly

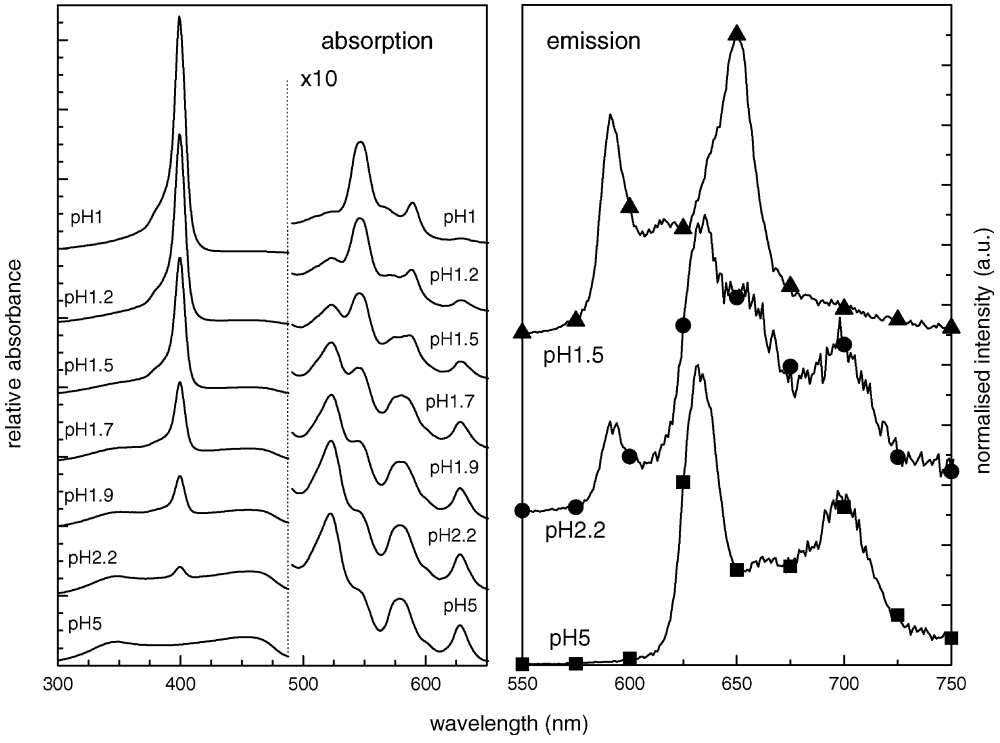

Fig. 2. Absorption and fluorescence spectra of MP in acidified aqueous solution for different pH values.

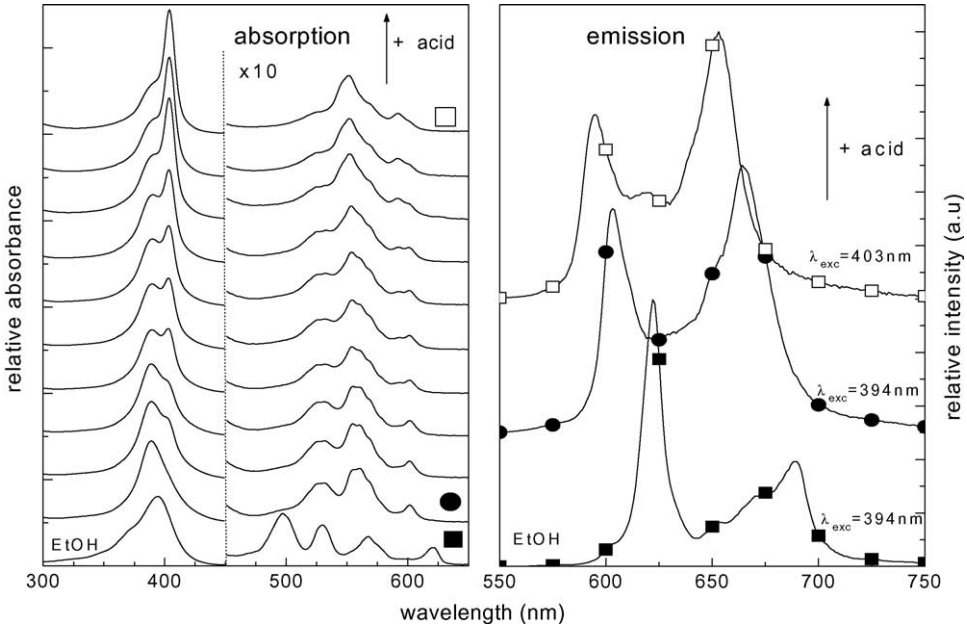

Fig. 3. Absorption and fluorescence of MP in ethanol with addition of acid (HCl) up until 5×10^{-3} M. (■) Representative of the spectra of the unionised form; (●) cation form; (□) dication form.

lower wavelengths than the former (but with the same appearance) we are confident in our attribution and relate the difference in wavelength to differences in dielectric constant of the medium.

The effect of acid addition on the fluorescence spectrum is also demonstrated in Fig. 2. This shows an overall shift to shorter wavelengths with acidification. New bands at 592 and 651 nm, related to the dication appear, while those at 632 and 700 nm diminish. This behaviour is similar to that reported for protoporphyrin IX on formation of a dication [11]. The spectrum obtained with the pH 5 solution is reminiscent of the neutral monomer, but not as sharp. This can be related to the presence of aggregates, such as dimers [18,20], manifest by the presence of a band around 665 nm. Some evidence for dimers also comes from comparing the absorption spectra (Fig. 2) with that calculated for this species [20]. There appears to be a similarity between the longer wavelength absorption bands, but our spectra differ in the lower wavelength *Q* region, which indicates a mixture of species, both aggregated and ionised.

The effect of adding acid or base was also verified using ethanol as a solvent and the corresponding absorption spectra are presented in Fig. 3. In pure ethanol the spectrum of the neutral monomer is clearly evident and on addition of small (sub-μl) quantities of acid (37% HCl) the transition to the cation, followed by the evolution to the dication is seen. This is plainly demonstrated in the fluorescence emission (Fig. 3) and also visible in the decay time data, which are given in Table 2, along with the decay time obtained using DMF for comparison. Analysis involving the decomposition of the spectrum in the *Soret* region was employed to follow the shape change in region with addition of acid (Fig. 4). This uncovered the existence of a band around 370 nm in pure ethanol, which disappears with the addition of the acid. The presence of neutral monomer absorption (393 nm) is seen throughout and the evolution of the ionised forms (404 nm

Table 2
Fluorescence lifetime data for MP in ethanol, with acid and base, and in DMF

Solvent	Acid/base	τ_1	τ_2	α_1	α_2	χ^2
DMF	–	15.3 ± 0.02		1		1.14
EtOH	Base	12.7 ± 0.02		1		1.17
	–	12.4 ± 0.05	7.1 ± 0.91	0.85	0.15	1.16
	+ Acid	12.5 ± 0.10	7.0 ± 0.15	0.70	0.30	1.05
	++ Acid	6.5 ± 0.08	2.7 ± 0.04	0.13	0.87	1.07

Lifetimes in ns.

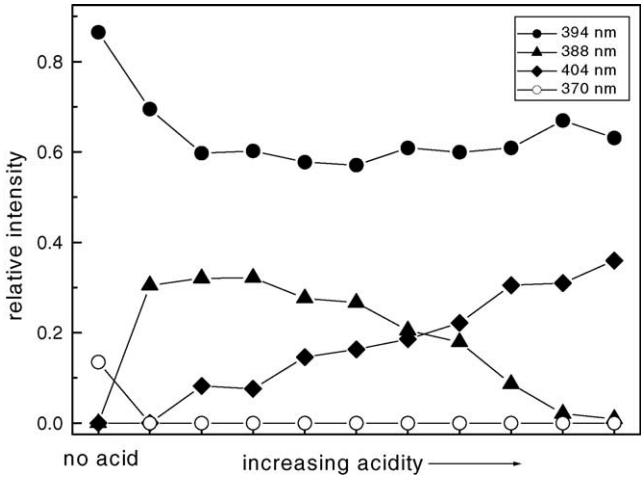

Fig. 4. Analysis of *Soret* region of MP in ethanol with the addition of acid. The acid concentration was increased until 5×10^{-3} M.

for cation, 389 nm for dication) with an increasing quantity of acid can be observed.

Looking at the time-resolved data, two components are required to fit the fluorescence decay of MP in pure ethanol. The long-lived (∼12.5 ns) is indicative of the neutral monomer [18] and the short-lived fluorescence (∼7 ns) is assigned to the cationic form, which is present on slight acidification and is unlikely to be related to dimers. On addition of a base (ammonia) to the ethanol solution the kinetics became monoexponential, with a decay time corresponding to that of the neutral form. Addition of acid to MP in ethanol at first produces an increase in the amount of the monocationic species and on the further addition of acid the decay is dominated by a short-lived fluorescence (∼3 ns), which we ascribe to the dication. At this point there is no component, which can be related to the neutral form. From our analysis it appears that each of the species present can be represented by a single exponential decay time. Another work on protonated metal free porphyrins, in this case H_4OEP^{2+} [22], found that a two component decay (with lifetimes, 1.5 and 3.3 ns) was required to fit the time-resolved data. In that study the authors said that the deactivation of the singlet state was affected by non-planar conformations, with a non-radiative contribution occurring via funnel points. In our case we do not observe the short component (1.5 ns) seen in that work, which may be related to the different substituent groups on the pyrrole ring and the solvents used in our study.

The effect of solvent on the steady state spectral properties of MP was also investigated in order to help elucidate the environment within the matrix interior and possible dye–host interactions. This was performed by measuring the absorption and emission spectra in a range of solvents (given in Table 1) with differing dielectric constants and refractive indices. In general the absorption spectra exhibited an *etio*-type structure of the *Q* bands (i.e. the intensity of band IV > III > II > I [21]) and the usual *Soret* band. The nomenclature of the four *Q* bands is such that on increasing wavelength band IV is encountered first, with band I at the longest wavelength [21] and they are related to the $Q_y(0, 1)$, $Q_y(0, 0)$, $Q_x(0, 1)$ and $Q_x(0, 0)$ transitions, respectively. In solvents, such as cyclohexane, dichloromethane and chloroform the *Q* bands exhibit a change in structure, similar to that seen in strongly acidified water, and in the case of chloroform a split in the *Soret* band (peaks present at 401 and 419 nm) accompanied by changes in the emission spectra (not shown) were observed. In the further analysis of the spectra only those exhibiting the *etio*-type *Q* band structure were chosen.

The four *Q* bands were analysed and compared to the behaviour of the *Soret* band (Fig. 5). As the gradients are lower than one it is clear that the wavelength of the *Soret* band is more solvent dependent than that of the *Q* bands. A similar treatment has been reported for tin(IV) mesoporphyrin [23], with a comparable outcome. However, the gradients we obtain are smaller with a significant difference found between the bands studied (0.25, 0.05, 0.21 and 0.25 for bands IV, III, II and I, respectively). Analysis applying the Mataga–Lippert equation [24] was not attempted because of the very small Stokes' shift between band I and the first emission band. Also functions taking into account the dielectric constant (ε), i.e. considering the redistribution of dipoles, did not yield satisfactory results. Analysis of the *Q* and *Soret* bands, by plotting against the refractive index function is

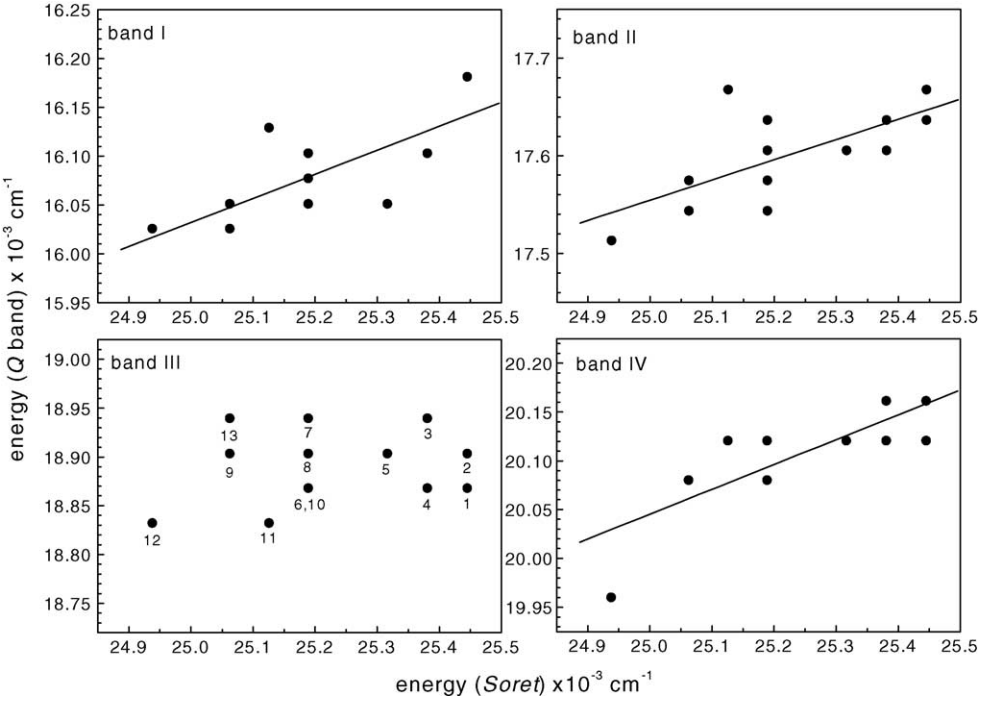

Fig. 5. Energy of the *Q* bands, against the *Soret* band energy for a variety of solvents (see Table 1 for details of solvent numbers illustrated for band III).

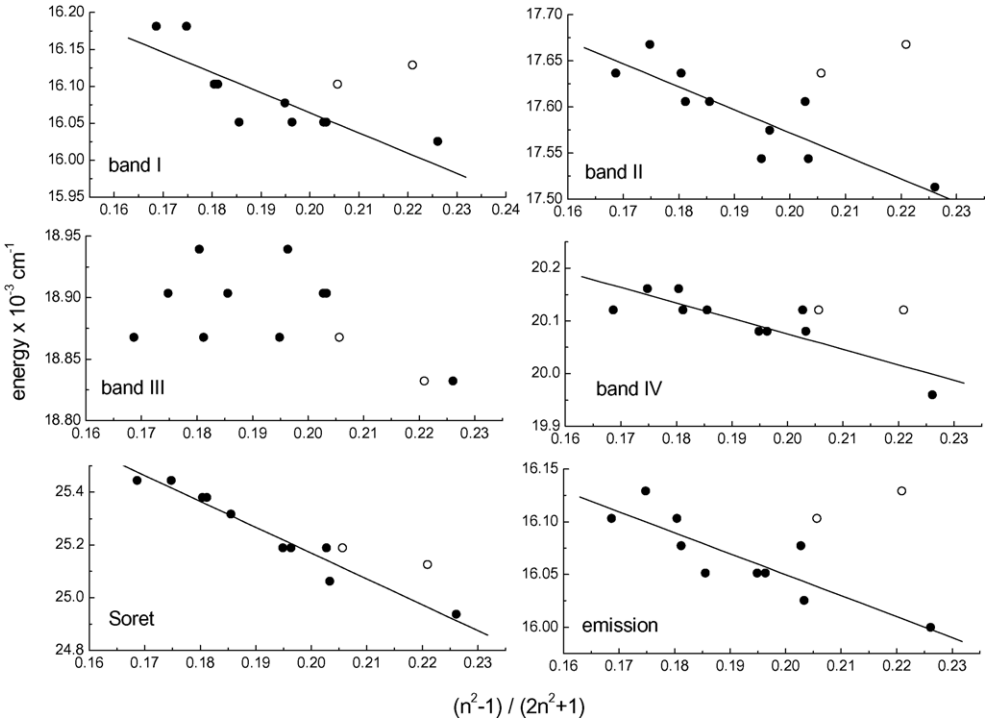

Fig. 6. Energy of the *Q* bands along with the *Soret* and main emission band, against $(n^2 - 1)/(2n^2 + 1)$ for a variety of solvents. The fits are made excluding DMF and DMSO (open circles).

given in Fig. 6. In all cases, considering all the points, at first sight the correlation for the *Q* bands appears worse than that obtained using the *Soret* band. However if the two aprotic solvents DMF and DMSO are neglected then, with the exception of band III, reasonable trends can be seen. The negative gradients for bands I, II and IV are 2.7, 2.5 and 2.9×10^3, respectively, although it should be noted that because of the relatively small shifts exhibited an appreciable error ($\pm 0.5 \times 10^3$) can be expected. The fact that a better fit is obtained when the aprotic solvents are neglected from the plot may be indicative of solvent interaction with the pyrrole core nitrogens. Band III does not appear to exhibit the same trend as the other bands with the refractive index function. This observation can relate to the fact band III gives a negative value in the polarization spectrum, while all the other bands show positive values [1]. Thus these transitions may be perturbed differently on changing the solvent. Our data (Fig. 6) exhibit no significant differences between absorption bands I, II and IV. With our selected range of solvents a shift in the peak emission of up to 5 nm was recorded, with a trend similar to that observed for the absorption bands (except band III).

A further treatment of both the absorption and emission (first band) was made by comparison of the band position with the $E_{T(30)}$ solvent scale from Reichardt's pyridinium betaine dye [25]. This scale has also been applied in the analysis of phthalocyanines [26]. The outcome of our treatment is presented in Fig. 7, which again displays differences between the absorption bands. In this case band III and the *Soret* band do not exhibit any discernable trend, while band IV appears in the whole unaffected by change of solvent. However, the other bands (I, II and main emission) show a similar behaviour, which is affected by the use of alcohols as solvents. These OH containing solvents effectively split the plots into two parts (the gradients are similar throughout, except for band I in alcohols which is approximately double) and again this demonstrates the sensitivity of MP to the presence (or absence) of protons.

3.2. Incorporation in sol–gel-derived matrices

The sol–gel reaction [13] does not instantly produce a solid matrix. In fact, although the reaction mixture may gel quickly (min) to form a usable medium to encapsulate selected molecules, the process of drying and aging to form the robust glassy matrix can take weeks or even months. Of course depending on usage it is possible to make use of the matrix at any point during this time and to add further dopants (even after gelling). Therefore we investigated the interaction of our chosen porphyrin with the TiO_2 sol–gel-derived matrix (at both the beginning and end of the matrix forming reaction), as well as in the final form of a SiO_2 sol–gel-derived monolith. Throughout the samples were measured at ambient temperatures and "initial" refers to when the reaction mixture has just gelled and "final" to an air stable glassy matrix, without any discernable structural changes occurring. Both types of monolith were produced with and without the addition of DMF, which we have previously employed within our matrices to alter the internal environment and to assist in the drying process [15].

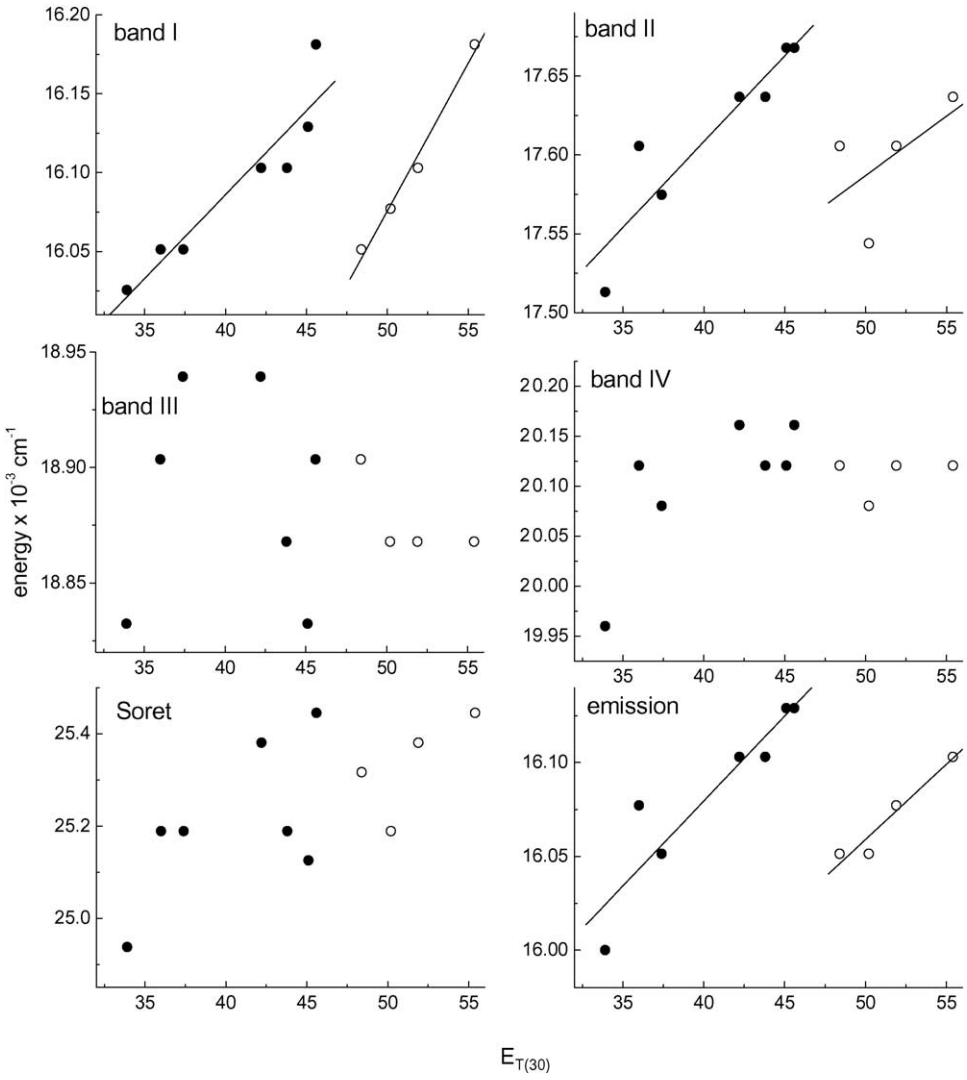

Fig. 7. Relation between absorption and fluorescence band position and the $E_{T(30)}$ solvent scale. The open circles represent alcohols.

The absorption spectra for the different samples are displayed in Fig. 8. In the *Soret* region for the TiO_2 samples the main band corresponds to that of the neutral monomer, although a shoulder on the longer wavelength side is also present. This is assigned to the presence of dication. Differences can be seen between the initial (more homogeneous) samples and the final glassy matrices. For the sample without DMF the structure in the *Q* region becomes less defined with aging and there is an apparent red shift in the bands. Because of the high level of absorption at lower wavelengths it was not possible to analyse the *Soret* region. Considering the MP in the SiO_2 matrices, we again see differences between the samples with and without DMF. In the presence of DMF the absorption spectrum in the *Q* region exhibits an *etio*-type structure (with bands at 497, 530, 567 and 620 nm), but with the presence of an extra band to the red at 650 nm, which may relate to the formation of a chlorin type photoproduct [27]. Further evidence for this assignment comes from the observation of this band for MP in DMF after prolonged irradiation. The four principal *Q* bands are at the same positions as those obtained in pure DMF, with the exception of band I, which has a 1 nm shift to the blue. Without DMF the spectrum of MP in the *Soret* region is that of the cation (peak at 387 nm) and this is also seen in the *Q* region.

Further information comes from the fluorescence spectra (presented in Fig. 9). Here two excitation wavelengths were employed (to preferentially excite different forms of MP) and for the initial TiO_2 samples the presence of both neutral monomer (peaks around 623 and 690 nm) and an ionised form (peaks around 600 and 656 nm) of MP were discerned. In the emission the peak wavelengths indicate that this ionised form is primarily the monocation, although from the absorption spectra it is known that the dication is also likely to be present. For the final forms of these matrices the picture is not so straightforward. For the sample with DMF, although both the neutral and dication forms are present, there is a broadening of the band around 650 nm, accompanied by a small shift to lower wavelengths. For the sample without DMF the

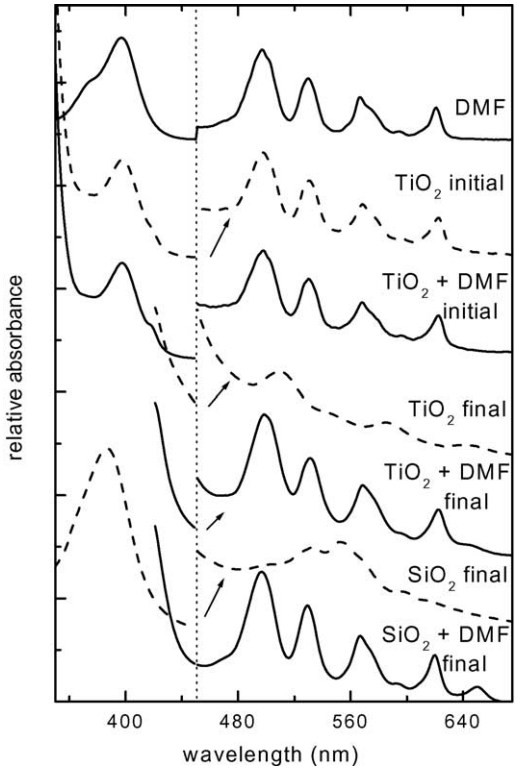

Fig. 8. Absorption spectra for MP in sol–gel-derived matrices, both with and without addition DMF. The absorption spectrum in DMF is given for comparison and the *Q* band region has been amplified for clarity.

differences are clearer, a peak close to 600 nm signals the presence of some dication and the spectrum is dominated by two broad bands close to 651 and 707 nm. The origin of these bands is hard to assign conclusively, but they are likely to have various roots, such as ionised and aggregated forms within the matrix structure. The emission structure is reminiscent of that obtained for microcrystalline meso-tetrakis (undecyl) porphyrin [28], although with a shift in wavelength. The presence of aggregates is not surprising because of the removal of solvents from the matrix during the drying and aging process. Another possibility is the presence of photoproducts, which can also contribute to the emission at 650 nm [27]. The silica sample with the addition of DMF ostensibly shows the emission of the neutral monomer, but with the existence of a band at 654 nm. Without the presence of additional solvent the emission spectra appears to be a combination of cation (in accordance with the absorption spectrum) and dication. The band positions for both absorption and emission spectra are summarised in Table 3.

From the time-resolved data for the silica matrices, given in Table 4, it is possible to assign the lifetimes to the different species. In the sample without DMF two decay components are recovered; 8.2 ns, the dominant decay which we assign to the cation and 4.1 ns, which we relate to the dication. These values are slightly longer than those obtained in acidified ethanol (Table 2). For MP in a silica matrix with DMF again some dication is manifest, as is the monomer, although with a longer decay time than in pure ethanol (12.7 ns) or with DMF (15.3 ns). The fluorescence decay of MP in degassed DMF was found to be monoexponential and a value of 19.4 ns was obtained from the analysis. The decay time of the neutral form in the silica matrix may therefore indicate a reduced oxygen concentration within the matrix. This also explains why the other decay components in these matrices are longer than those observed in aerated solution. The major fluorescing species in the matrix with DMF has a decay time ∼1 ns, which we assign to the band at 650 nm. The origin of this band may relate to aggregates and/or photoproducts [18,27]. The assignment of the decay components of MP in the titania matrices is slightly more complex. Overall four different decay times are recovered for MP present in the sol–gel-derived matrices; a long-lived decay (13–17 ns) easily related to the neutral monomeric form, a shorter decay (∼5–8 ns) assigned to the cation, a decay of ∼2.5 ns ascertaining to the dication and a significant proportion of a short-lived (1 ns) component.

Table 3
Band positions of MP incorporated into sol–gel-derived matrices

System	Stage	*Soret* region	*Q* region	Emission
TiO_2	Initial	25.13	20.08, 18.83, 17.61, 16.05	16.05, 14.49[a]
				16.69, 16.05, 15.24, 14.49[b]
	Final	–	19.65, 17.09, 15.55	16.58, 15.36, 14.16[c]
				16.61, 15.36, 14.12[d]
TiO_2 + DMF	Initial	25.19	20.08, 18.87, 17.61, 16.05	16.08, 14.51[a]
				16.67, 16.08, 15.24, 14.49[b]
	Final	–	20.04, 18.83, 17.57, 16.05	16.08, 15.34, 14.53[a]
				16.58, 16.05, 15.27, 14.51[e]
SiO_2	Final	25.84	18.80, 18.12, 16.78	17.21, 16.64, 15.13
SiO_2 + DMF	Final	–	20.12, 18.90, 17.64, 16.13, 15.38	16.03, 15.29, 14.56

Energies in cm^{-1} ($\times 10^{-3}$). Note because of the large absorption in some samples the *Soret* band position was not determined and for the emission the main discernable bands are given.

[a] Excitation was at 397 nm.
[b] Excitation was at 419 nm.
[c] Excitation was at 418 nm.
[d] Excitation was at 510 nm.
[e] Excitation was at 421 nm.

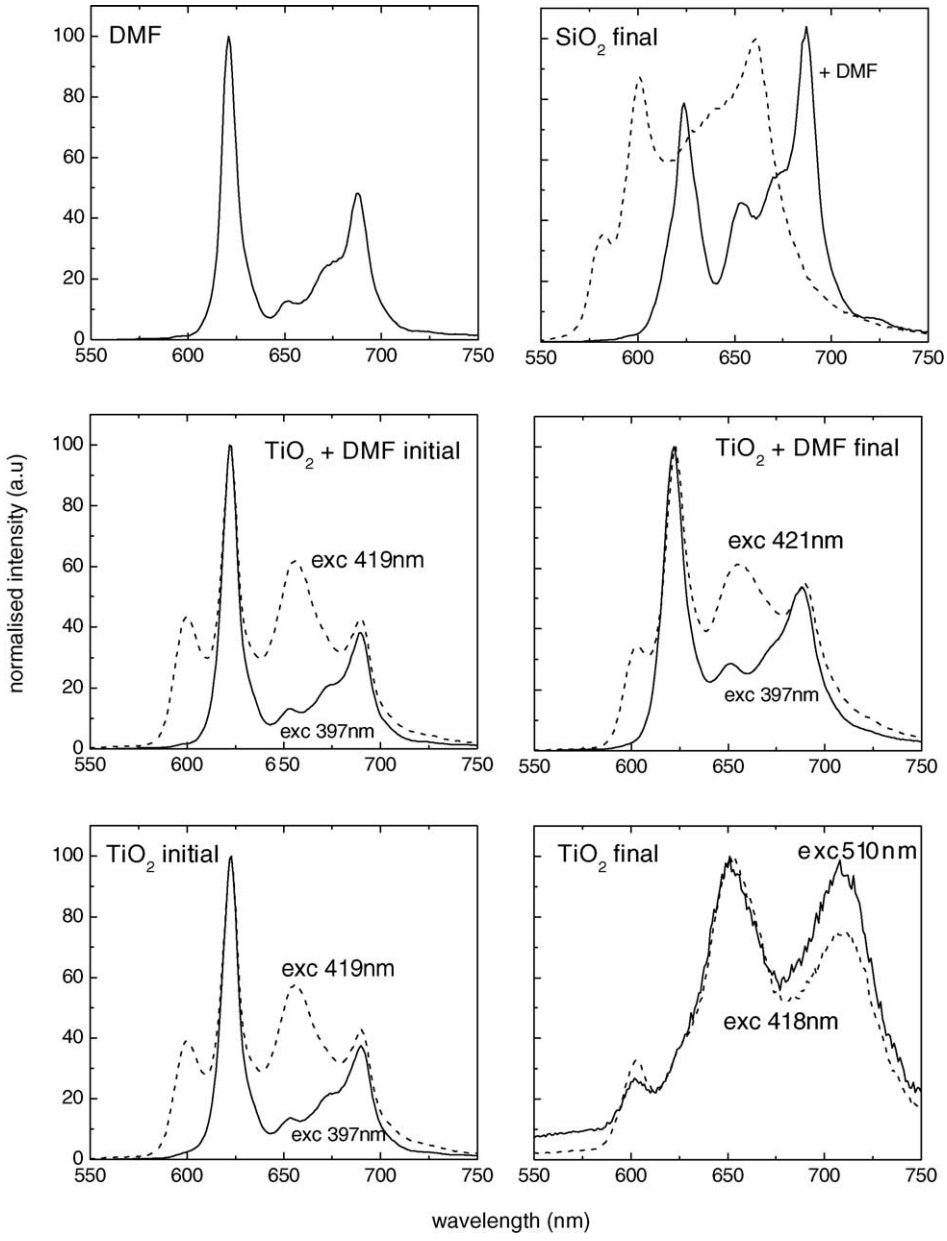

Fig. 9. Initial and final emission spectra for MP in TiO_2 and SiO_2 sol–gel-derived matrices. That in pure DMF is given for comparison.

Table 4
Fluorescence lifetime data for MP incorporated in sol–gel-derived matrices

System	Stage	τ_1	τ_2	τ_3	α_1	α_2	α_3	χ^2
TiO_2	Initial	13.9 ± 0.08	6.2 ± 0.58	1.0 ± 0.04	0.32	0.17	0.51	1.06
	Intermediate	8.4 ± 0.16	2.7 ± 0.21	0.6 ± 0.01	0.03	0.10	0.87	1.18
	Final	6.4 ± 0.17	2.2 ± 0.33	0.5 ± 0.01	0.02	0.06	0.92	1.13
TiO_2 + DMF	Initial	14.7 ± 0.04	5.8 ± 0.51		0.84	0.16		1.13
	Intermediate	16.1 ± 0.09	5.4 ± 0.42	1.0 ± 0.12	0.37	0.30	0.33	1.07
	Final	12.9 ± 0.15	5.4 ± 0.11	1.6 ± 0.14	0.11	0.55	0.34	1.06
SiO_2	Final	8.2 ± 0.07	4.1 ± 0.53		0.71	0.29		1.05
SiO_2 + DMF	Final	17.2 ± 0.12	4.5 ± 0.15	1.1 ± 0.03	0.12	0.34	0.54	1.12

Lifetimes in ns.

It is clear that the relative quantity of the neutral form decreases with aging and that in the DMF containing sample it is accompanied by an increase in the ionised form and short-lived fluorescent species. With the other titania matrix a faster decrease in both neutral monomer and ionised forms is observed and most of the fluorescence originates from the shorter-lived species. This can be explained by MP solvated in the retained solvent within the matrix pore structure (as we have found for Nile Red [15]). In the sample without DMF there is a greater interaction with the bulk oxide material and a reduction in solubility can favour the formation of aggregates, which can be the cause of the short-lived emission.

In order to elucidate further information concerning the interaction of MP with the matrix and any retained solvents the band positions of the neutral form, mainly those of absorption band I and the principal emission (see Table 2) were analysed. An estimate for the refractive index sensed by the porphyrin was made by comparing to the solution study (Fig. 6). Refractive index values of 1.43 and 1.35 were found for the titania and silica matrices, respectively. These compare with 1.9, which we have previously calculated for our titania matrix (in thin film form) [29] and 1.45 generally found for silica. However they are close to those expected from solvents that could be encountered in the matrix structure. This is further evidence that it is unlikely that the porphyrin is incorporated within the bulk oxide material, but resides inside the pore structure of the matrix, with the possibility of the presence of retained solvent. A comparison with the $E_{T(30)}$ scale was also performed, considering both solvent groups, i.e. alcohols and others. Unsurprisingly, when analysed using the absorption data, no difference is observed between the two forms of the titania matrix at the initial stage (it should be noted that the quantity of DMF present is relatively small) and $E_{T(30)}$ values of 37 and 49 (for alcohols) obtained. Similar values were obtained for the final form of the TiO_2 matrix with DMF. These values compare with 44 and 53, respectively, obtained for the final form of the silica matrix with DMF. However, if analysis is performed using the emission spectrum of MP in the silica matrix comparable values are obtained. A difference between the $E_{T(30)}$ values obtained from both absorption and emission data are encountered for the DMF containing samples pointing to further influence of the retained solvent, which requires further investigation.

These results indicate that the MP experiences slightly different environments within the pore structure of the different matrix forms. In the initially formed titania matrices the porphyrin senses a similar environment and a significant proportion exists as the neutral monomer, especially in the matrix with DMF, which moderates the effect of the acid catalyst. Without this retained solvent more of the ionised (both cation and dication) MP is present. The quantity of the neutral form reduces with time and without the presence of DMF the spectrum of MP within the titania monolith broadens and shifts to the red accompanied by a decrease of the fluorescence lifetime. With DMF this dramatic effect is not observed on the same timescale, although the amount of neutral monomer is reduced and the presence of some aggregates (plus photoproducts) as well as ionised MP is probable. The final forms of the silica matrices also exhibit the effect of adding DMF. Without this solvent the main form of MP is the cation, while various forms are present in the DMF containing matrix. This can be related to various environments encountered within the matrix interior.

4. Summary

Both in solution and microheterogeneous sol–gel-derived matrices we have found evidence for the presence of various forms of mesoporphyrin IX. In pure solvents the spectral band positions are affected by the presence of acid, resulting in ionised forms of MP, each with their characteristic spectrum and fluorescence decay time. A dependency of both absorption and emission band position on solvent refractive index and $E_{T(30)}$ are observed. Although the spectral shifts are small, since trends exist for both forms of analysis we believe they are significant. The solution data assists in interpreting the interactions of the porphyrin when it is introduced into various forms of sol–gel-derived matrices. Here the moderating effect of additional DMF is noted, although on long timescales (many months) for the titania matrices MP appears in an aggregated form (possibly also with photoproducts) which then disappears, possibly by some interaction with the matrix material. The silica matrices do not exhibit this effect, although the existence of both ionised forms and photoproducts can be ascertained.

References

[1] G.P. Gurinovich, A.N. Sevchenko, K.N. Solov'ev, Sov. Phys. Uspekhi. 6 (1963) 67.
[2] M. Gouterman, in: D. Dolphin (Ed.), The Porphyrins, vol. III, Academic Press, 1978, p. 1.
[3] K.M. Kadish, K.M. Smith, R. Guilard (Eds.), The Porphyrin Handbook, vol. 1–10, Academic Press, 2000.
[4] M. Ochsner, J. Photochem. Photobiol. B: Biol. 39 (1997) 1.
[5] M. Stefanidou, A. Tosca, G. Themelis, E. Vazgiouraki, C. Balas, Eur. J. Dermatol. 10 (2000) 351.
[6] F. Ricchelli, J. Photochem. Photobiol. 29 (1995) 109.
[7] A. Kay, M. Grätzel, J. Phys. Chem. 97 (1993) 6272.
[8] A. Kay, R. Humphry-Baker, M. Grätzel, J. Phys. Chem. 98 (1994) 952.
[9] M. Kępczyński, R.P. Pandian, K.M. Smith, B. Ehrenberg, Photochem. Photobiol. 76 (2002) 127–134.
[10] I. Bárdos-Nagy, R. Galántai, A.D. Kaposi, J. Fidy, Int. J. Pharmaceut. 175 (1998) 255.
[11] A.P. Savitski, E.V. Vorobyova, I.V. Berezin, N.N. Ugarova, J. Coll. Interf. Sci. 84 (1981) 175.
[12] M. Kępczyński, B. Ehrenberg, Photochem. Photobiol. 76 (2002) 486.
[13] C.J. Brinker, G.W. Scherer, Sol–Gel Science: The Physics and Chemistry of Sol–Gel Processing, Academic Press, 1990.
[14] G. Hungerford, M.R. Pereira, J.A. Ferreira, T.M.R. Viseu, A.F. Coelho, M.I.C. Ferreira, K. Suhling, J. Fluoresc. 3–4 (2002) 397.
[15] G. Hungerford, J.A. Ferreira, J. Luminesc. 93 (2001) 155.
[16] K.K. Flora, J.D. Brennan, J. Phys. Chem. B 105 (2001) 12003.

[17] Y. Tachibana, S.A. Haque, I.P. Mecer, J.R. Durrant, D.R. Klug, J. Phys. Chem. B 104 (2000) 1198.
[18] B. Roeder, H. Wabnitz, J. Photochem. Photobiol. B: Biol. 1 (1987) 103.
[19] R. Margalit, M. Rotenberg, Biochem. J. 219 (1984) 445.
[20] P. Abós, C. Artigas, S. Bertolotti, S.E. Braslavsky, P. Fors, K. Lang, S. Nonell, F.J. Rodríguez, M.L. Sesé, F.R. Trull, J. Photochem. Photobiol. B: Biol. 41 (1997) 53.
[21] K.M. Smith (Ed.), Porphyrins and Metalloporphyrins, Elsevier, 1975.
[22] V.S. Chirvony, A. Van Hoek, V.A. Galievsky, I.V. Sazanovich, T.J. Schaafsma, D. Holten, J. Phys. Chem. B 104 (2000) 9909.
[23] Y. Chen, B. Zhang, J-G. Chen, D-Y. Huang, Spectrochim. Acta A 57 (2001) 2451.
[24] N. Mataga, T. Kubota, Molecular, Interactions and Molecular spectra, Marcel Dekker, Inc., New York, 1970.
[25] C. Reichardt, Chem. Rev. 94 (1994) 2319.
[26] H. Weitman, S. Schatz, H.E. Gottlieb, N. Kobayashi, B. Ehrenberg, Photochem. Photobiol. 73 (2001) 473.
[27] R. Bonnett, G. Martínez, Tetrahedron 57 (2001) 9513.
[28] H.D. Burrows, A.M. Rocha Gonsalves, M.L.P. Leitão, M.daG. Miguel, M.M. Pereira, Supremol. Sci. 4 (1997) 241.
[29] T.M.R. Viseu, G. Hungerford, M.I.C. Ferreira, J. Phys. Chem. B 106 (2002) 1853.